Supporting Information

Tumor-Mitochondria Dual Targeted Aza-BODIPY-based Nanotheranostic Agent for Multimodal Imaging-Guided Phototherapy

Dapeng Chen,[a] Jiaojiao Zhang,[a] Yunyun Tang,[a] Xiaoyu Huang,[a] Jinjun Shao,[a] Weili Si,[a] Jun Ji,[c] Qi Zhang,[d*] Wei Huang,[a,b] Xiaochen Dong[a*]*

[a]Key Laboratory of Flexible Electronics (KLOFE) and Institute of Advanced Materials (IAM), Nanjing Tech University (NanjingTech), Nanjing 211800, China.

E-mail: iamxcdong@njtech.edu.cn

[b]Shaanxi Institute of Flexible Electronics (SIFE), Northwestern Polytechnical University (NPU), 127 West Youyi Road, Xi'an 710072, China

[c]Nanjing Stomatological Hospital, Medical School of Nanjing University, Nanjing 210008, PR China.

E-mail: drjijun@hotmail.com

[d]School of Pharmaceutical Sciences, Nanjing Tech University (NanjingTech), 30 South Puzhu Road, Nanjing 211800, China.

E-mail: zhangqi@njtech.edu.cn

1. Materials and Reagents

3,4-Dimethoxybenzaldehyde, 4-methoxyacetophenone, boron trifluoride etherate, folic acid, (2-carboxyethyl) triphenylphosphonium bromide, N-bromo-succinimide (NBS), 1,3-diphenylisobenzofuran (DPBF), methylene blue (MB) were purchased from Adamas-beta® (Shanghai, China). mPEG-NH_2 (molecular weight: 5000) was purchased from Shanghai Yarebio Co. Ltd. Other chemical agents were purchased from Shanghai Lingfeng Chemical Reagent Co. Ltd. All the chemical agents are used as received.

2. Characterization

Nuclear magnetic resonance (NMR) spectra were measured by using a Bruker Ultra Shield Plus. GC-MS was recorded on a Shimadzu GC-MS-QP 2010 Plus mass spectrometer. MALDI-TOF-MASS (Matrix-assisted laser desorption/ionization time of flight mass spectrometry) was performed on a Bruker antoflex speed MALDI-TOF for data acquisition. The UV-visible absorption was recorded by UV-3600 Shimadzu UV-vis-NIR spectrometer (Shimadzu, Japan). Fluorescence spectra were recorded by an F-4600 spectrofluorophotometer (Hitachi, Japan). An E50 infrared camera (FLIR, Arlington, VA) was employed to record photothermal images. The confocal fluorescence images were obtained by an Olympus IX 70 inverted microscope (Olympus, Japan).

3. Supplemental Methods

3.1. Synthesis and Characterization of MeOABBr

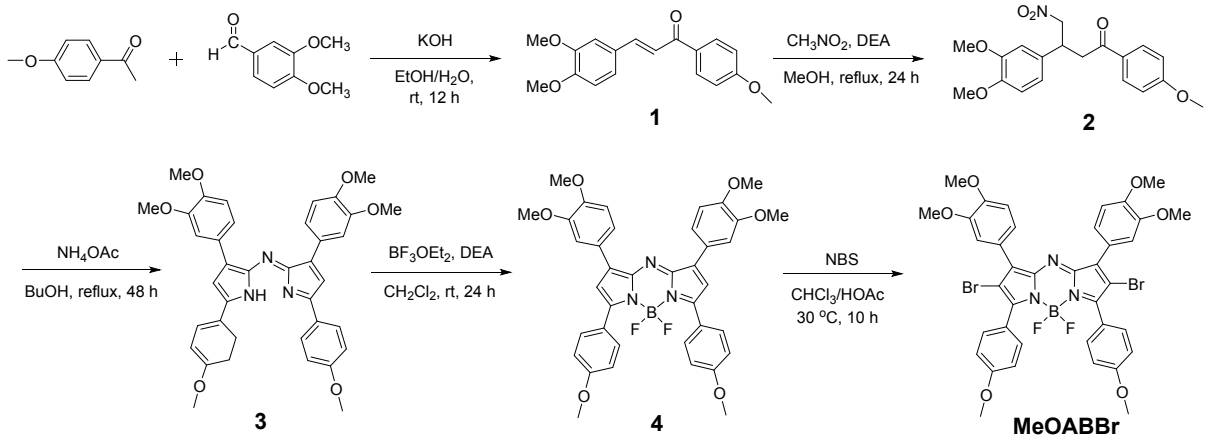

Scheme **S1** Synthetic routes for **MeOABBr**

1-(4-methoxylphenyl)-3-(3,4-dimethoxyphenyl)prop-2-en-1-one (1)

3,4-Dimethoxybenzaldehyde (6.647 g, 0.04 mol), 4-methoxyacetophenone (6.007 g, 0.04 mol) and KOH (0.224 g, 0.004 mol) were dissolved in ethanol/H_2O (85:15 v/v, 80 mL) and stirred at room temperature for 24 h. The crude product was filtered as yellow precipitate (10.740 g, 90%). ^{1}H NMR (500 MHz, $CDCl_3$): δ ppm 8.09 (d, J = 9.0 Hz, 2H, Ar-H), 7.81 (d, J = 6.5 Hz, 1H, CH-C=O), 7.46 (d, J = 15.5 Hz, 1H, Ar-CH=), 7.20 (d, J = 6.5 Hz, 1H, Ar-H), 7.04 (d, J = 9 Hz, 2H, Ar-H) 6.95 (d, J = 8.5 Hz, 1H, Ar-H), 4.00 (s, 3H, OCH_3), 3.97 (s, 3H, OCH_3), 3.93 (s, 3H, OCH_3), ^{13}C NMR (500 MHz, $CDCl_3$): δ ppm 188.71, 163.28, 151.31, 149.29, 144.06 131.35, 130.68, 128.12, 122.90, 119.90, 113.78, 111.23, 110/28, 55.97, 55.43. ESI MS (m/z): calcd for [$C_{18}H_{18}O_4$ + H], 299.1; found 299.1.

1-(4-methoxyphenyl)-3-(3,4-dimethoxyphenyl)-4-nitrobutan-1-one (2)

Product **1** (5.971 g, 0.02 mol), nitromethane (6.050 g, 0.1 mol) and diethylamine (7.317 g, 0.1 mol) was dissolved in 100 mL of methanol and heated under reflux for 24 h After cooling down, acidified with 2 M diluted hydrochloric acid, extracted with CH_2Cl_2, and

evaporated to give the dark orange oily crude product. The crude product was further purified by chromatography on silica gel eluting with CH_2Cl_2/petroleum ether (1:5) to give the white product (3.522 g, 49%). ^{1}H NMR (500 MHz, $CDCl_3$): δ ppm 7.94 (d, J = 8.5 Hz, 2H, Ar-H), 6.97 (d, J = 8.5 Hz, 2H, Ar-H), 6.85 (d, J = 14.5 Hz, 3H, Ar-H), 4.86 (dd, J = 6.5, 12 Hz, 1H, CH_2-NO_2), 4.72 (dd, J = 8.0, 12.0 Hz, 1H, CH_2-NO_2), 4.2 (m, 1H, CH), 3.90 (s, 6H, OCH3), 3.87 (s, 3H, OCH_3), 3.42 (m, 2H, O=C-CH_2) ^{13}C NMR (500 MHz, $CDCl_3$): δ ppm 195.39, 163.74, 149.16, 148.15, 131.72, 130.23, 129.49, 119.18, 113.78, 111.57, 111.08, 79.72, 55.87, 55.77, 55.38, 41.22, 39.16. ESI MS (m/z): calcd for [$C_{19}H_{21}NO_6$ + Na], 382.1; found 382.1.

[5-(4-methoxyphenyl)-3-(3,4-dimethoxyphenyl)-1H-pyrrol-2-yl][5-(4-methoxyphenyl)-3-(3,4-dimethoxyphenyl) pyrrol-2-ylidene] amine (3)

Product **2** (1.797 g, 0.005 mol), acemonium acetate (15.42, 0.2 mol) and butanol (100 mL) were added into a 250 mL round-bottom flask and heated under reflux for 48 h. After cooling down, the precipitate was purified by chemotography on silica gel eluting with CH_2Cl_2/petroleum ether (1:1.5) to give the dark brown product (1.390 g, 44%). ^{1}H NMR (500 MHz, $CDCl_3$): δ ppm 7.79 (d, J = 10.5 Hz, 4H, Ar-H), 7.54 (dd, J = 2.5, 10.5 Hz, 2H, Ar-H), 7.47 (d, J = 2.5 Hz, 2H, Ar-H), 6.96 (s, 2H, pyrrole-H), 6.94 (d, J = 6.5 Hz, 4H, Ar-H), 6.85 (d, J = 10.5 Hz, 2H, Ar-H), 3.92 (s, 6H, OCH_3), 3.84 (s, 6H, OCH_3), 3.73 (s, 6H, OCH_3). NH was not observed. ^{13}C NMR (500 MHz, $CDCl_3$): δ ppm 161.18, 153.96, 149.30, 149.16, 148.83, 142.13, 128.03, 127.31, 125.15, 121.90, 114.59, 113.41, 112.50, 111.10, 56.00, 55.83, 55.44. ESI MS (m/z): calcd for [$C_{38}H_{37}N_3O_6$], 631.3; found 631.2.

BF_2 Chelate of [5-(4-methoxyphenyl)-3-(3,4-dimethoxyphenyl)-1H-pyrrol-2-yl] [5-(4-methoxyphenyl)-3-(3,4-dimethoxyphenyl) pyrrol-2-ylidene] amine (4)

Compound **3** (0.632 g, 1 mmol) and diisopropylethylamine (1.16 g, 9 mmol) was dissolved in dried CH_2Cl_2 (100 mL) under nitrogen atmosphere. Boron trifluoride diethyl etherate (1.7 g, 12 mmol) was added and stirred at room temperature for 24 h. The solution was washed with deionized water. Finally, the organic layer was collected, dried, evaporated, and purified to give the purple product (0.556 g, 82%). ^{1}H NMR (500 MHz, $CDCl_3$): δ ppm 8.08(d, J = 11 Hz, 4H, Ar-H), 7.65 (d, J = 2.5, 10.5 Hz, 2H, Ar-H), 7.54 (d, J = 2 Hz, 2H, Ar-H), 7.00 (s, 2H, pyrrole-H), 6.98 (s, 2H, Ar-H), 6.94 (d, J = 11 Hz, 4H, Ar-H), 3.95 (s, 6H, OCH3), 3.87 (s, 6H, OCH_3), 3.81 (s, 6H, OCH_3). ^{13}C NMR (500 MHz, $CDCl_3$): δ ppm 161.78, 157.74, 150.41, 149.10, 145.22, 143.408, 143.17, 131.50, 125.92, 124.33, 122.61, 117.65, 114.17, 112.47, 111.24, 56.03, 55.94, 55.37. ESI MS (m/z): calcd for $[C_{38}H_{34}BF_2N_3O_6 + H]/2$, 339.1; found 339.1.

BF_2 Chelate of [4-bromo-5-(4-methoxyphenyl)-3-(3,4-dimethoxy phenyl)-1H-pyrrol-2-yl] [5-(4- methoxyphenyl)-3-(3,4-dimethoxyphenyl) pyrrol-2-ylidene] amine (MeOA BBr)

Compound **4** (0.271 g, 0.40 mmol) and N-bromo-succinimide (178 mg, 1 mmol) were dissolved in chloroform and acetic acid solution and stirred for 12 h. The reaction mixture was washed with sodium thiosulphate and sodium bicarbonate solution, and then extracted with chloroform. The organic layer was dried over Na_2SO_4 and evaporated under reduced pressure to obtain the product as dark blue solid (0.301 g, 90%). ^{1}H NMR (500 MHz, $CDCl_3$): δ ppm 7.71(d, J = 11.5 Hz, 4H, Ar-H), 7.53 (d, J = 13 Hz, 2H, Ar-H), 7.38 (s, 2H,

Ar-H), 7.02 (m, 6H, Ar-H), 3.99 (s, 6H, OCH_3), 3.90 (s, 6H, OCH_3), 3.74 (s, 6H, OCH_3). ^{13}C NMR (500 MHz, $CDCl_3$): δ ppm 168.48, 161.63, 160.33, 157.27, 150.54, 148.55, 144.06, 132.37, 127.17, 125.52, 124.23, 122.00, 114.20, 113.07, 110.65, 55.98, 55.77, 55.29. MALDI-TOF MS (m/z): calcd for $C_{38}H_{32}BBr_2F_2N_3O_6$, 833.07; found 833.47.

3.2. Singlet oxygen detection of MeOABBr

Singlet oxygen quantum yields (Φ_Δ) of **MeOABBr** were measured with MB as standard (Φ_Δ = 0.57 in DCM)[1]. The solution containing **MeOABBr** and DPBF were irradiated with 660 nm laser for 30 s. The oxidation decrease of DPBF's absorption at 418 nm was monitored by UV-vis-NIR spectrophotometer. Thereafter, Φ_Δ was calculated according to **Equation S1**[2]:

$$\Phi_\Delta = \Phi_{\Delta(std)} \times \frac{S_{sam}}{S_{std}} \times \frac{F_{std}}{F_{sam}} \qquad \textbf{(S1)}$$

where '*sam*' and '*std*' represent **MeOABBr** and MB, respectively. *S* represents the slope of the absorbance of DPBF at 418 nm versus irradiation time, *F* represents the absorption correction factor, which is given by $F = 1 - 10^{-O.D.}$.

3.3. Photothermal effect of FMAB NPs

The solution of **FMAB** NPs with different concentration (10, 20 and 50 μg/mL, equivalent to the concentration of **MeOABBr**) in PBS solution were irradiated with 730-nm laser (1 W cm^{-2}) for 12 min. The temperature was recorded by FLIR thermal camera. Photothermal conversion efficiency (η) of **FMAB** NPs solution was measured under the irradiation of 730-nm laser at power density of 1 W cm^{-2}. DI water was used as the control group. The real-time temperature change was recorded using a FLIR thermal camera. Then η was calculated according to **Equation S2** and **S3**[3]:

$$\eta = \frac{hS\Delta T_{\max} - Q_s}{I(1-10^{-A_{730}})} \qquad \textbf{(S2)}$$

$$\tau_s = \frac{m_D C_D}{hS} \qquad \textbf{(S3)}$$

where h denotes the coefficient of heat transfer, S is container's surface area, and the value of hS is calculated from the Figure S4b. ΔT_{max} represents temperature change of **FMAB** NPs aqueous solution at the maximal steady-state temperature, and I is laser power. A_{730} is the absorbance intensity of **FMAB** NPs at 730 nm and Q_s expresses the heat associated with light absorption by the solvent. τ_s represents the time constant of sample-system. C_D and m_D are heat capacity and mass (4.2 J g^{-1}) of the solvent H_2O, respectively.

4. Supplemental figures

(a)

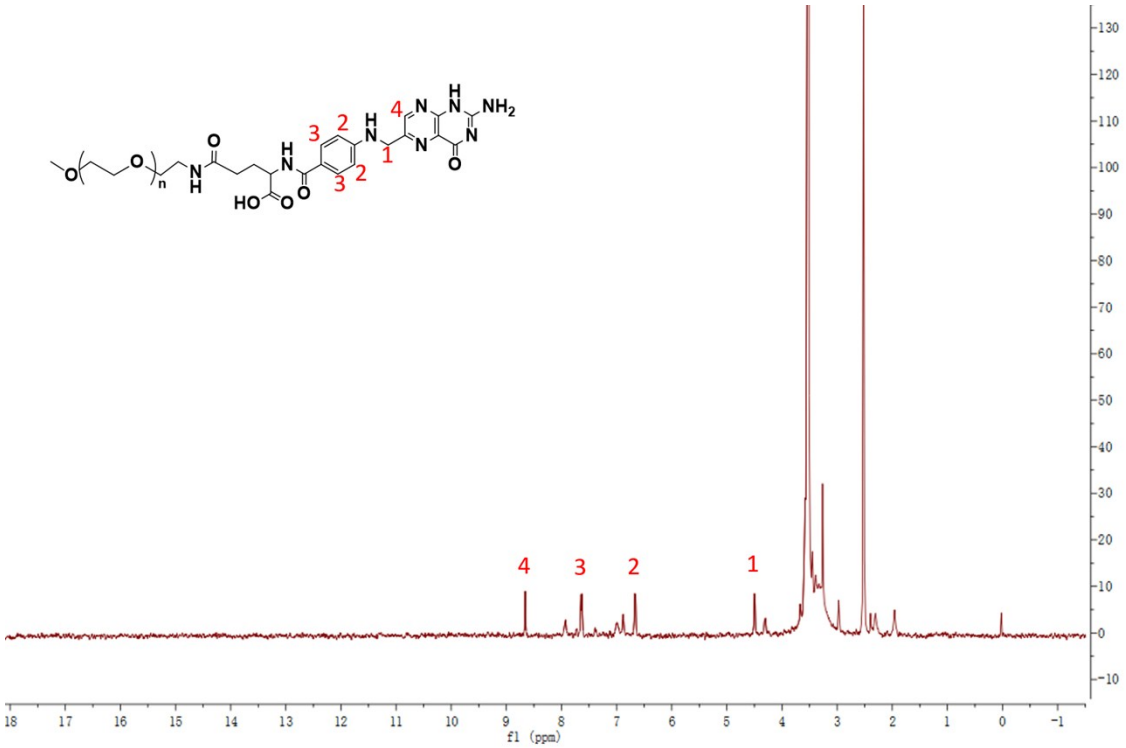

(b)

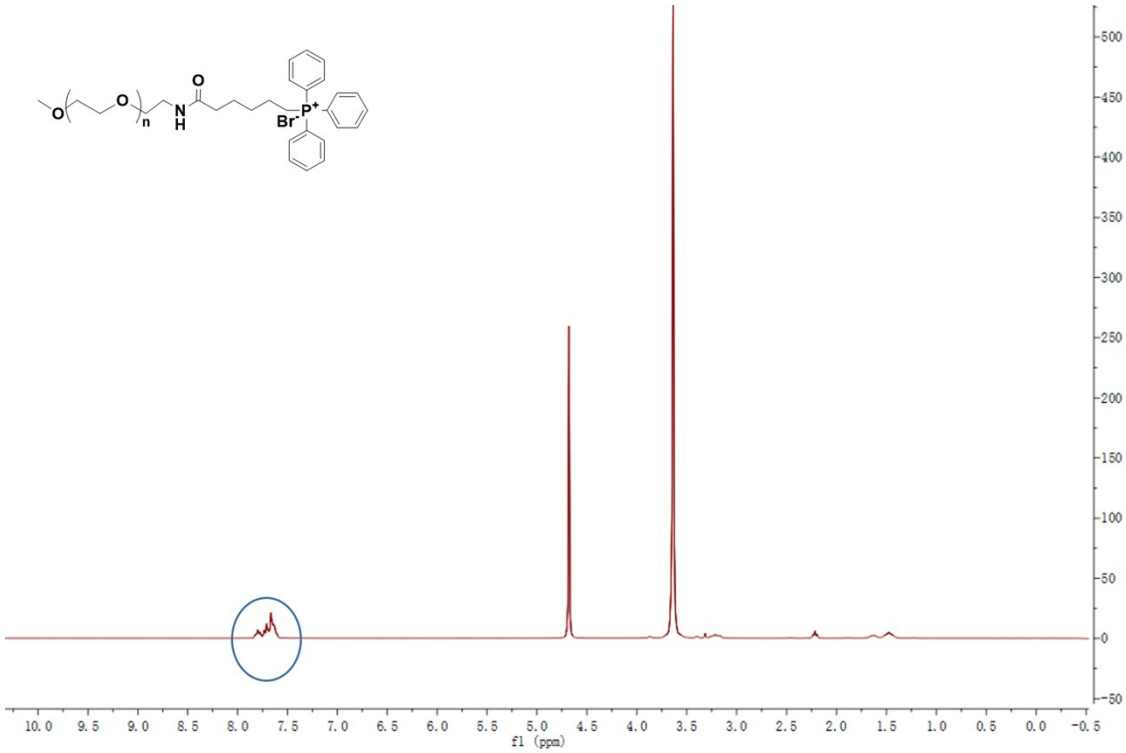

Figure S1 (a) ^{1}H NMR spectrum of PEG-FA; (b) ^{1}H spectrum of PEG-TPP.

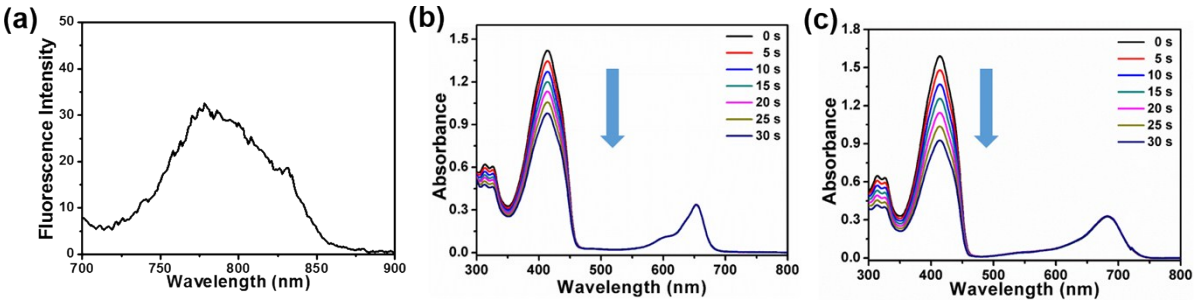

Figure S2 (a) Fluorescence spectrum of **FMAB** NPs. (b) UV-vis absorption spectra of DPBF solution incubated with MB in dichloromethane upon irradiation with 660-nm laser for different time. (c) UV-vis absorption spectra of DPBF solution incubated with **MeOABBr** in dichloromethane upon irradiation with 660-nm laser for different time.

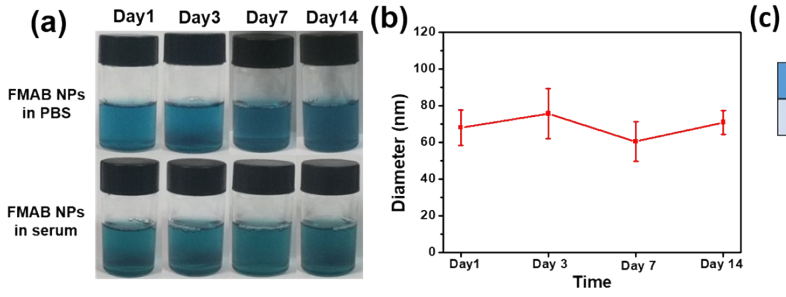

Sample	Zeta Potential (mV)
FMAB NPs	5.6±2.3

Figure S3 (a) Photographs of **FMAB** NPs in PBS and serum solution for different days. (b) Size change of **FMAB** NPs in PBS for different days. (c) Zeta potential of FMAB NPs.

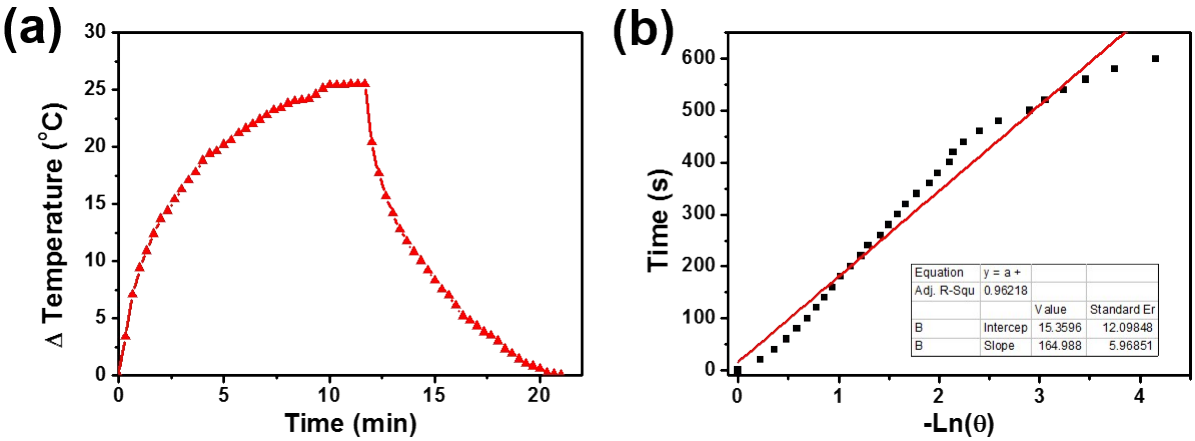

Figure S4 (a) Photothermal effect of **FMAB** NPs solution with 730-nm laser (1 W cm^{-2}). (b) Time constant is measured to be τ_s = 164.988 s, in which the linear time data from cooling period was applied versus negative natural logarithm of driving force temperature.

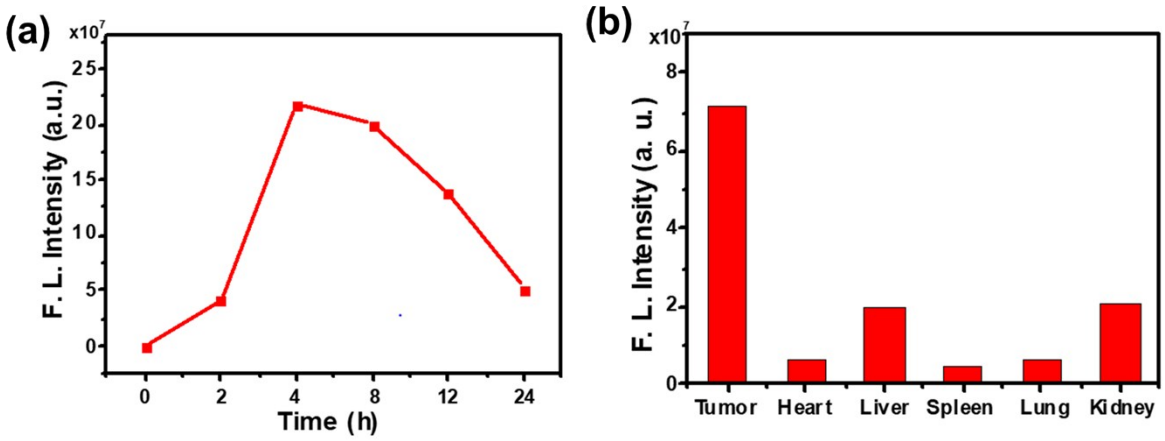

Figure S5 (a) Fluorescence intensity changes of **FMAB** NPs in tumor sites at different time. (b) Fluorescence intensity of **FMAB** NPs in tumor and normal organs.

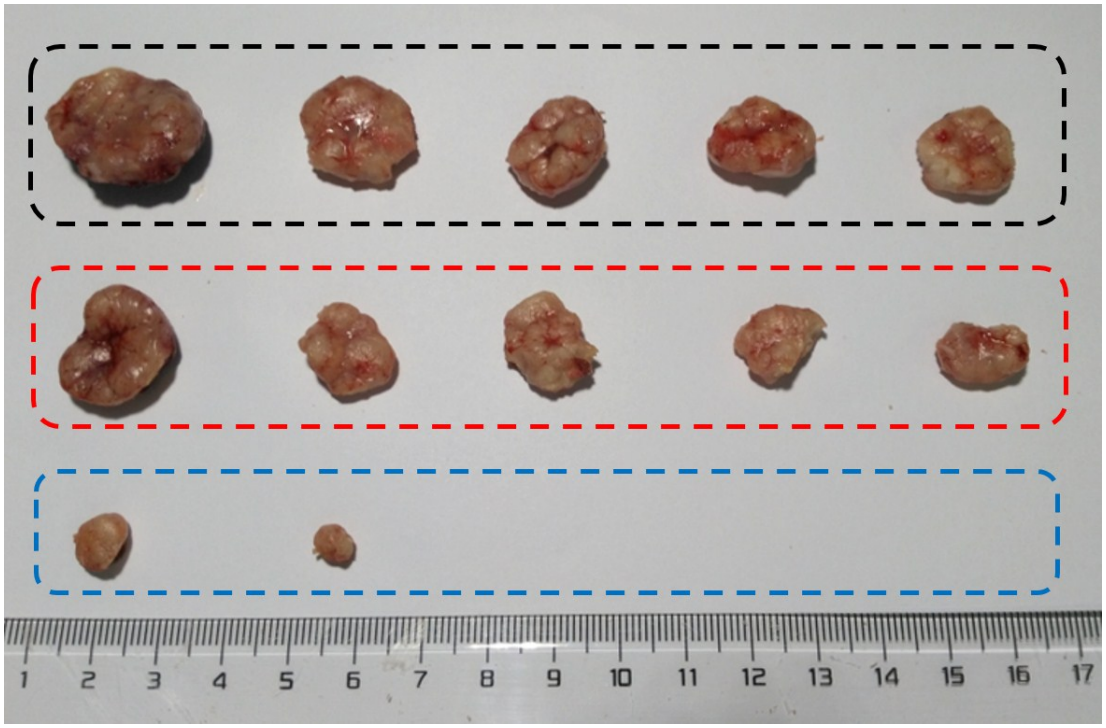

Figure S6 Photo images of tumors collected from mice treated with PBS (black dash line, **FMAB** NPs (red dash line), **FMAB** NPs + irradiation (blue dash line).

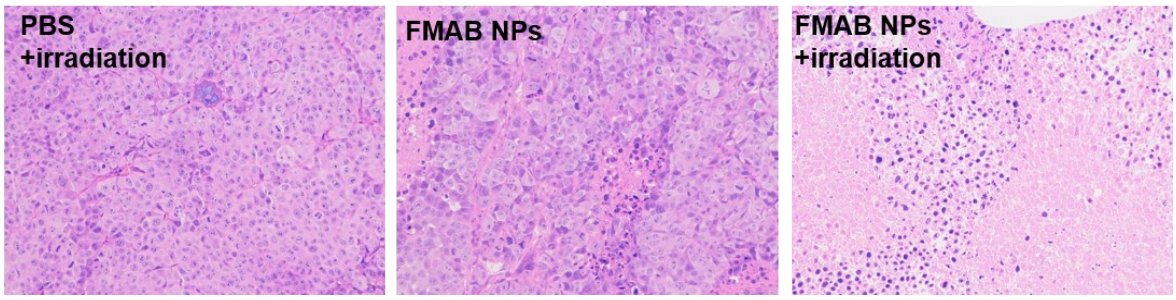

Figure S7 H&E staining examination of tumors for different groups after 18 days of treatments.

Supplemental References

1. S. Guo, L. Ma, J. Zhao, B. Kucukoz, A. Karatay, M. Hayvali, H. G. Yaglioglu and A. Elmali, *Chem. Sci.*, 2014, **5**, 489-500

2. Q. Tang, W. Xiao, C. Huang, W. Si, J. Shao, W. Huang, P. Chen, Q. Zhang and X. Dong, *Chem. Mater.*, 2017, **29**, 5216-5224.

3. D. Chen, Q. Tang, J. Zou, X. Yang, W. Huang, Q. Zhang, J. Shao and X. Dong, *Adv. Healthcare Mater.*, 2018, **7**, 1272-1281.